Citation
Zhang, S. and Ferrie, S. and Peiris, C.R. and Lyu, X. and Vogel, Y.B. and Darwish, N. and Ciampi, S. 2021. Common Background Signals in Voltammograms of Crystalline Silicon Electrodes are Reversible Silica-Silicon Redox Chemistry at Highly Conductive Surface Sites. Journal of the American Chemical Society. 143 (3): pp. 1267-1272. http://doi.org/10.1021/jacs.0c10713

Common Background Signals in Voltammograms of Crystalline Silicon Electrodes are Reversible Silica–Silicon Redox Chemistry at Highly Conductive Surface Sites

Song Zhang, Stuart Ferrie, Chandramalika R. Peiris, Yan B. Vogel, Nadim Darwish, Simone Ciampi*

ABSTRACT: The electrochemical reduction of bulk silica, due to its high electrical resistance, is of limited viability, namely requiring temperatures in the excess 850 °C. By means of electrochemical, and electrical measurements in atomic force microscopy, we demonstrate that at a buried interface, where silica has grown on highly conductive Si(110) crystal facets, the silica–silicon conversion becomes reversible at room temperature and accessible within a narrow potential window. We conclude that parasitic signals commonly observed in voltammograms of silicon electrodes originate from silica–silicon redox chemistry. While these findings do not remove the requirement of high temperature towards bulk silica electrochemical reduction, they however redefine for silicon the potential window free from parasitic signals, and as such, significantly restrict the conditions where electroanalytical methods can be applied to the study of silicon surface reactivity.

Cyclic voltammetry still reigns as the main form of electrochemical spectroscopy.[1] From electro-catalysis, to sensing and corrosion, this straightforward current–potential measurement is a widespread tool for studying redox reactions at solid–liquid interfaces.[2] For both metals and semiconductors,[3-6] and for diffusive and diffusion-less systems,[7-9] kinetic, mass transport and thermodynamic parameters of redox reactions are readily obtained from the analysis of voltammetric currents (peak positions and intensities).[10]

Owing to the simplicity of recording current magnitude against time – charges – chemists and surface scientists routinely turn to Coulomb values extracted from cyclic voltammograms to monitor the progress and estimate yields of surface reactions.[9, 11-15] Even the chemisorption of just enough molecules to results in a fractional monolayer (e.g. <0.1 ng cm^{-2}) generally leads to currents well above the noise of basic commercial potentiostats.[16-18] This aspect makes voltammetry one of the most sensitive analytical techniques for studying the reactivity of surfaces.[19]

Silicon remains the technologically most relevant semiconductor, and research is constantly expanding the pool of reactions targeting its surface.[20, 21] However, the power of voltammetry, when applied to silicon surface science, hinges around a correct understanding of background current signals. While for platinum, gold and carbon, all common adventitious voltammetric signals have been explained and assigned,[22] recurrent parasitic signals observed for silicon electrodes remain unexplained.

Several published reports, dealing with the surface reactivity of silicon crystals, carry clear evidence of a pair of adventitious redox waves, either disregarded as artifacts, or often tentatively associated with the adsorption of a target molecule.[9, 23-26] Herein we demonstrate how to systematically reproduce and amplify this parasitic signal. We bring evidence of this signal being the reversible electrochemical conversion of silica to silicon, taking place at the buried silicon–silica interface in correspondence of ubiquitous highly conductive crystal defects.

Figure 1 illustrates the process of deliberately oxidizing a monolayer-coated, oxide-free,[27] Si(111) surface in aqueous 1.0 M $HClO_4$. This is an exceedingly common electrode–electrolyte system for silicon electrochemistry,[28-30] and when we first ramped the voltage, from −0.5 V to a relatively low anodic vertex of 0.0 V, nothing unexpected appeared in the current trace (Figure 1a). Raising the anodic vertex from 0.0 to 1.0 V led again, at a first look, to a featureless voltammogram, with the only exception of a steep rise in current which is generally associated with the oxidation of either the substrate or the solvent (Figure 1b). However, a closer inspection of the trace in Figure 1b indicates the appearance of a surface-confined cathodic wave, labelled as **1** in the return segment of the first cycle (Figure 1c). This wave is coupled to a new anodic signal, evident in the third segment (**2**). These new signals increase in size, and shift anodically, upon further cycling (waves labelled as **3**–**5** in Figure 1c). These waves are therefore associated with anodic damaging of the electrode, that is, the appearance of silica on its surface. Figure S1 shows the changes in the XPS Si 2p narrow scan after the anodic process, revealing the appearance of a photoemission at binding energy of 102 eV, which is assigned to SiO_X species.[31] From the above results we infer that the background reversible redox peaks, of which we are trying to define the origin, are most likely related to silicon oxides. This is surprising, since the reduction of silica requires normally very harsh conditions (high temperatures and molten salts electrolytes, *vide infra*).[32-34] Further, these waves reflect an irreversible chemical change of the electrode, as opposed to a simple capacitive process. Data in Figure S2 show that the surface-confined redox couple formed upon the anodic excursion to 1.0 V is remarkably stable to prolonged potential cycling. Its surface density, estimated under the assumption of a one-

electron redox reaction,[35, 36] is of (2.34 ± 0.68) × 10^{-12} mol cm^{-2}, which is equivalent to about 0.1% of the surface atoms density of an ideal Si(111) surface (15.66 × 10^{14} atoms cm^{-2}).

This last quantitative remark is important, since this

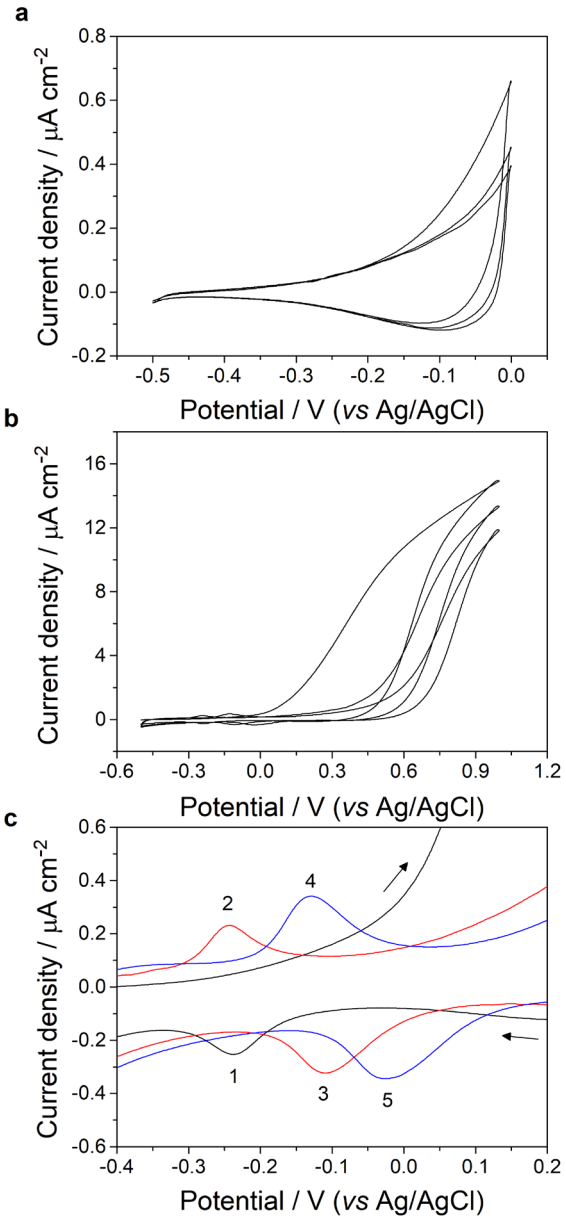

Figure 1. Cyclic voltammograms of 1,8-nonadiyne-modified Si(111) electrodes. The electrode voltage is ramped from an initial −0.5 V to an anodic vertex, set to either 0.0 V in (a), or to 1.0 V in (b). (c) Color-coded magnified views of the first three sequential voltammetric cycles (six segments) shown in (b). The voltage scan rate is 0.1 V/s, and the electrolyte is aqueous 1.0 M $HClO_4$.

fractional coverage is close to the ratio, expected for a Si(111) wafer, of atoms on step-edges to atoms on surface terraces. There is in fact a strong dependence between the electrical conductivity of a silicon surface and its crystal orientation.[37] Recently published electrical measurements, performed with microscopic tungsten probes, have revealed that the electrical conductivity for common low-index silicon facets decrease in the order (110)>>(111)>(100).[37] We have observed similar facet-dependent conductivity trends in small Cu_2O crystals.[38] We therefore postulate that the electrical conductivity of the silicon–SiO_X interface is enhanced at sites where silica grows on surface defects of large conductivity.[37] Under

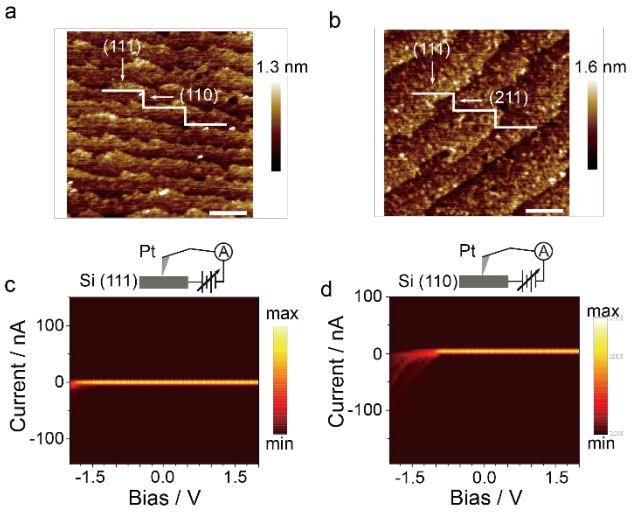

Figure 2. (a,b) Atomic force microscopy height images of monolayer-coated Si(111) wafers. Topography images were aquired paying attention to ensure a parallel alignment between the major flat, indicating the [110] direction, and the x-direction of the AFM raster scan. Steps between terraces are either roughly parallel to the sample major flat (a), or oriented 30° away from it (b). Scale bars in (a) and (b) are 400 and 220 nm, respectively. (c,d) Heat maps of current–potential (I–V) data for platinum–silicon junctions acquired by conductive AFM on Si(111) and Si(110) surfaces. I–V curves are sampled at 100 evenly spaced points and are recorded at a constant force of 2.5 μN with a 100 nA/V sensitivity. The sample-to-tip bias routing is such that forward currents appear in the negative quadrant, that is, when the n-type silicon is biased negative with respect to the platinum AFM tip

these circumstances the silica–silicon redox couple may become reversible within a moderate potential window, therefore explaining the origin of the parasitic signals ubiquitous to oxidized silicon electrodes (Figure 1).

We therefore investigated the existence of highly conductive defects on nominal single-crystal silicon wafers. Atomically flat electrodes are an idealization, and well-prepared and nominally flat semiconductor electrodes are a continuous of flat terraces separated by small vertical steps.[5, 39] Atomic force microscopy (AFM) topography data in Figure 2a and 2b indicate that on Si(111) electrodes – a crystal cut commonly used by electrochemists and surface scientists[40, 41] – these vertical steps tend to have preferred orientations. Commercial Si(111) wafers have a major flat indicating the [110] direction (a stereographic view of a Si(111) wafer is in Figure S3). Surface topography data obtained by AFM reveal that these vertical steps form angles of either approximately 0° or 30° with respect to the direction of the major flat (Figure 2a and 2b). Steps separating Si(111) terraces are therefore principally exposing (110) and (211) planes. An analysis of step heights and terrace widths in the AFM topography images (e.g. Figure 2a) revealed that even in high quality samples, such as those in Figure 2, the surface area ratio of Si(110) to

Si(111) is 0.19 ± 0.05 to 100. This percentage is in striking accordance with the 0.1% surface coverage, estimated above by cyclic voltammetry, for the adventitious redox couple appearing upon oxidation to the silicon electrode (Figure 1). Representative AFM height profiles, acquired along a direction normal to the predominant step direction, and used to estimate the area ratio of (110) and (211) facetes to (111) terraces in nominal Si(111) wafers, are in Figure S4.

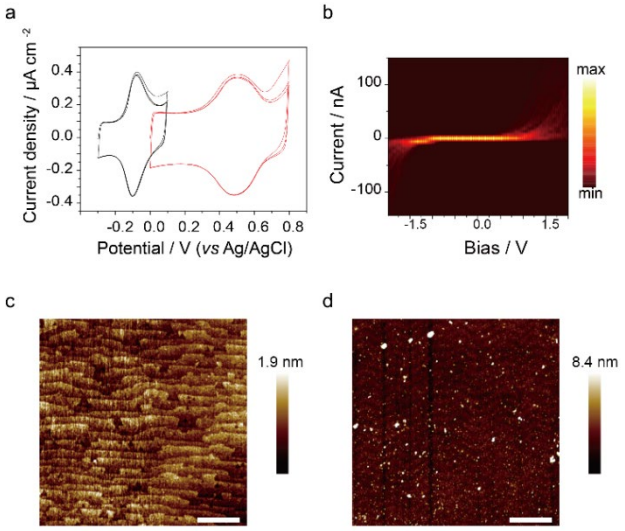

Figure 3. (a) Cyclic voltammograms of Si(111) electrodes indicating an anodic shift with progressive potential cycling (three cycles, black curves; 100 cycles, red curves) of the apparent formal potential of the silica/silicon redox couple. The scan rate is 0.1 V/s, and the electrolyte is 1.0 M $HClO_4$. b) I–V curves (AFM) of platinum–silicon junctions recorded on anodically damaged Si(111) electrodes, showing a significant increase in the leakage current (positive quadrant) compared to fresh samples (Figure 2c). (c,d) Changes to surface topography before (c) and after (d) three potential sweeps between −0.5 V and 1.0 V (0.1 V/s, 1.0 M $HClO_4$). Scale bars in (c) and (d) are 1 μm.

It was therefore relevant to test the relative conductivity of Si(110) and Si(111) facets. Current–potential data (I–V hereafter), acquired by conductive AFM (Figure 2c and 2d, and Figures S5 and S6), indicate that the conductivity of Si(110) wafers is significantly larger than that of Si(111). For example, at a forward bias of −1.5 V, the current of platinum–Si(110) junctions is on average 21 times larger (−48 nA versus only −2.20 nA) than that of junctions made to Si(111). Silicon has no conductive bulk oxide phases,[32] and the electro-reduction of silica has only been demonstrated in $CaCl_2$ melts.[34, 42] By ensuring good mobility of O^{2-} anions the high-temperature melt aids the de-oxidation of SiO_2.[32, 42] However, under an electric field, oxygenated anions (O^{2-} and OH^-) are known to migrate across a thin silica layer, even at room temperature.[43-45] Further, the growth of silica over an oxide-free substrate introduces energy levels in the band gap,[46] demonstrated indirectly by a sharp drop of the anodization voltage observed as soon as silica adlayers form over a silicon electrode.[46-49]

We therefore propose that despite the low electrical conductivity of bulk silica,[32, 34, 50] its electrochemical reduction at the silica–silicon interface becomes apparently reversible at highly-conductive facets, and manifests in both aqueous (Figure 1 and Figure S7a–c) as well as non-aqueoues electrolytes (Figure S7d–e). It has been suggested that the mobile species migrating across the thickening oxide film are mainly anions.[51] Water molecules enter the first layers of the oxide and dissociate into ionic species, which then migrate toward the silicon/oxide interface under the effect of the electrical field in the oxide.[43, 46] The apparent formal potential of this parasitic redox couple

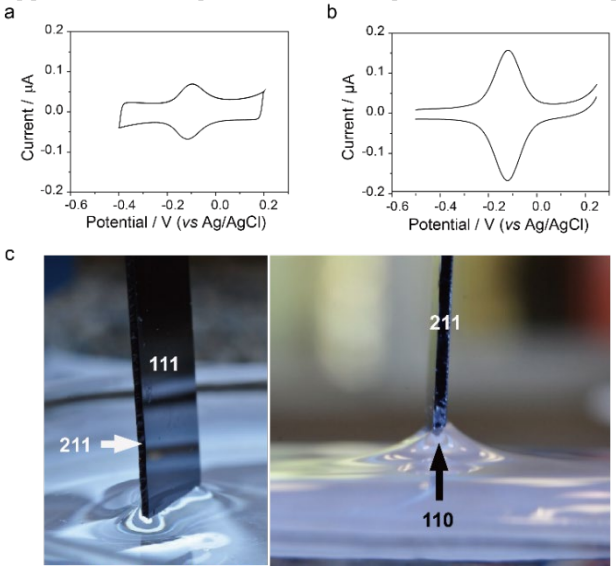

Figure 4. (a,b) Cyclic voltammograms of anodically damaged Si(111) and Si(110). The surface coverage of the redox background signal observed on Si(110) is 12.73 $\times 10^{-12}$ mol cm^{-2}, which is 6.9 times larger than on Si(111). The geometric area ratio of the two electrodes is approximately 1.9 ((111) to (110), estimated by capacitance measurements). Voltammograms were recorded at a scan rate of 0.1 V/s, in aqueous 1.0 M $HClO_4$, after three potential sweeps (0.1 V/s) between −0.5 V and 1.0 V. (c) Optical images of the hanging-meniscus configuration used to wet the (110) facet in a three-electrode experiment used to record the voltammograms in (b). A graphical depiction of the (211) and (110) crystal directions in commercial Si(111) wafer is in Figure S13.

shifts anodically with progressive oxidation (Figure 3a), which reflects a similar shift for the electrode open circuit potential. These shifts are caused by an increase, with oxidation, of the dark leakage current.[5, 6] I–V curves shown in Figure 3b (and in Figure S8) confirm a substantial increase in leakage current upon initial substrate oxidation. Our oxidation-induced redox background couple is therefore in series with a "leaky" silica-rich diode. As expected, the sharp and regular terraced structure of the etched and monolyer-coated Si(111) surface(Figure 3c) disappears after oxidation: the highly conductive (110) and (211) step edges have been covered by an oxide layer (Figure 3d, Figure S9).

To further confirm that the surprising silica/silicon redox reversibility arises from the silica adlayer sitting on highly conductive silicon sites, we performed electrochemical experiments on macroscopic samples cleaved to expose mainly (110) planes. This was done by cutting a Si(111) wafer along a direction parallel to the supplier-marked lap (Figure 4c). The wafer was then etched and chemically

passivated, before dipping it in the electrolyte so to wet only the (110) face. As shown in Figure 4, voltammograms acquired on anodically damaged Si(110) leads to redox waves significantly larger (ca. 6.9 fold) than on Si(111).

We note that bias-driven adsorption of ions,[19] as a potential contributor to the parasitic redox signal, was ruled out (Figure S7). Furthermore, surface coverages and peak positions do not change with pH, indicating that the new couple formed after anodic damaging of the surface is the result of a charge transfer not coupled to proton transfer (Figure S10). Controls with amorphous silicon,[38] as well as with non-silicon conductors (Figure S11), indicated no appearance of redox signals after an anodic over-oxidation process, reinforcing that this new surface-confined redox couple relates to the crystalline structure of the silicon surface.

In conclusion, we have explored the origin of a recurrent cyclic voltammetry background signal found in a widespread semiconductor laboratory system – Si(111) electrodes. An oxidative damage, deliberate or not, of common single crystal silicon Si(111) and Si(100) electrodes (Figure S12) leads to the appearance of a specific set of voltammetric waves. This current signal is the reversible silica/silicon redox process, occurring on highly conductive steps separating (111) terraces. This finding has immediate implications in the electrochemistry, and surface chemistry, of silicon, effectively restricting the potential window that is free from parasitic signals and therefore permitting the study of surface reactions by means of electroanalytical methods.

ASSOCIATED CONTENT

Supporting Information

Experimental section, stereographic projections, additional AFM (conductive and topography), x-ray photoelectron spectroscopy, and cyclic voltammetry data. This material is available free of charge via the Internet at http://pubs.acs.org

AUTHOR INFORMATION

Corresponding Author

Simone Ciampi – *School of Molecular and Life Sciences, Curtin Institute of Functional Molecules and Interfaces, Curtin University, Bentley, Western Australia 6102, Australia.*
Email*:* simone.ciampi@curtin.edu.au

Authors

Song Zhang, Stuart Ferrie, Chandramalika R. Peiris, Yan B. Vogel, Nadim Darwish – *School of Molecular and Life Sciences, Curtin Institute of Functional Molecules and Interfaces, Curtin University, Bentley, Western Australia 6102, Australia.*

Notes

The authors declare no competing financial interest.

ACKNOWLEDGMENTS

S.C. and N.D. acknowledge support from the Australian Research Council (grants no. DP190100735 and FT190100148).

REFERENCES

(1) Heinze, J., Cyclic Voltammetry—"Electrochemical Spectroscopy". New Analytical Methods (25). *Angew. Chem. Int. Ed.* **1984**, *23*, 831–847.

(2) Nicholson, R. S., Theory and Application of Cyclic Voltammetry for Measurement of Electrode Reaction Kinetics. *Anal. Chem.* **1965**, *37*, 1351–1355.

(3) Santangelo, P. G.; Miskelly, G. M.; Lewis, N. S., Cyclic Voltammetry at Semiconductor Photoelectrodes. 1. Ideal Surface-Attached Redox Couples with Ideal Semiconductor Behavior. *J. Phys. Chem.* **1988**, *92*, 6359-6367.

(4) Weber, K.; Creager, S. E., Voltammetry of Redox-Active Groups Irreversibly Adsorbed onto Electrodes. Treatment Using the Marcus Relation between Rate and Overpotential. *Anal. Chem.* **1994**, *66*, 3164-3172.

(5) Vogel, Y. B.; Zhang, L.; Darwish, N.; Gonçales, V. R.; Le Brun, A.; Gooding, J. J.; Molina, A.; Wallace, G. G.; Coote, M. L.; Gonzalez, J.; Ciampi, S., Reproducible Flaws Unveil Electrostatic Aspects of Semiconductor Electrochemistry. *Nat. Commun.* **2017**, *8*, 2066.

(6) Vogel, Y. B.; Molina, A.; Gonzalez, J.; Ciampi, S., Quantitative Analysis of Cyclic Voltammetry of Redox Monolayers Adsorbed on Semiconductors: Isolating Electrode Kinetics, Lateral Interactions, and Diode Currents. *Anal. Chem.* **2019**, *91*, 5929-5937.

(7) Laviron, E., The Use of Linear Potential Sweep Voltammetry and of A.C. Voltammetry for the Study of the Surface Electrochemical Reaction of Strongly Adsorbed Systems and of Redox Modified Electrodes. *J. Electroanal. Chem.* **1979**, *100*, 263-270.

(8) Laviron, E., Surface Linear Potential Sweep Voltammetry: Equation of the Peaks for a Reversible Reaction When Interactions between the Adsorbed Molecules Are Taken into Account. *J. Electroanal. Chem. Interf. Electrochem.* **1974**, *52*, 395-402.

(9) Zhang, L.; Laborda, E.; Darwish, N.; Noble, B. B.; Tyrell, J.; Pluczyk, S.; Brun, A. P. L.; Wallace, G. G.; Gonzalez, J.; Coote, M. L.; Ciampi, S., Electrochemical and Electrostatic Cleavage of Alkoxyamines. *J. Am. Chem. Soc.* **2018**, *140*, 766–774.

(10) Compton, R. G.; Banks, E. C., *Understanding Voltammetry*. Imperial College Press, Covent Garden, London, UK, **2011**.

(11) Kwon, Y.; Mrksich, M., Dependence of the Rate of an Interfacial Diels-Alder Reaction on the Steric Environment of the Immobilized Dienophile: An Example of Enthalpy-Entropy Compensation. *J. Am. Chem. Soc.* **2002**, *124*, 806-812.

(12) Yeap, W. S.; Murib, M. S.; Cuypers, W.; Liu, X.; van Grinsven, B.; Ameloot, M.; Fahlman, M.; Wagner, P.; Maes, W.; Haenen, K., Boron-Doped Diamond Functionalization by an Electrografting/Alkyne–Azide Click Chemistry Sequence. *ChemElectroChem* **2014**, *1*, 1145-1154.

(13) Hu, Q.; Deng, X.; Kong, J.; Dong, Y.; Liu, Q.; Zhang, X., Simple and Fast Electrochemical Detection of Sequence-Specific DNA Via Click Chemistry-Mediated Labeling of Hairpin DNA Probes with Ethynylferrocene. *Analyst* **2015**, *140*, 4154-4161.

(14) Fabre, B., Functionalization of Oxide-Free Silicon Surfaces with Redox-Active Assemblies. *Chem. Rev.* **2016**, *116*, 4808–4849.

(15) Peiris, C. R.; Vogel, Y. B.; Le Brun, A. P.; Aragones, A. C.; Coote, M. L.; Diez-Perez, I.; Ciampi, S.; Darwish, N., Metal-Single-Molecule-Semiconductor Junctions Formed by a Radical Reaction Bridging Gold and Silicon Electrodes. *J. Am. Chem. Soc.* **2019**, *141*, 14788–14797.

(16) Wei, J.; Liu, H.; Dick, A. R.; Yamamoto, H.; He, Y.; Waldeck, D. H., Direct Wiring of Cytochrome C's Heme Unit to an Electrode: Electrochemical Studies. *J. Am. Chem. Soc.* **2002**, *124*, 9591-9599.

(17) Rohde, R. D.; Agnew, H. D.; Yeo, W. S.; Bailey, R. C.; Heath, J. R., A Non-Oxidative Approach toward Chemically and Electrochemically Functionalizing Si(111). *J. Am. Chem. Soc.* **2006**, *128*, 9518–9525.

(18) Ciampi, S.; James, M.; Le Saux, G.; Gaus, K.; Justin Gooding, J., Electrochemical "Switching" of Si(100) Modular Assemblies. *J. Am. Chem. Soc.* **2012**, *134*, 844–847.

(19) Gileadi, E., *Electrode Kinetics for Chemists, Chemical Engineers and Materials Scientists*. Wiley-VCH Verlag GmbH, New York, **1993**, p 597.

(20) Ciampi, S.; Harper, J. B.; Gooding, J. J., Wet Chemical Routes to the Assembly of Organic Monolayers on Silicon Surfaces Via the Formation of Si−C Bonds: Surface Preparation, Passivation and Functionalization. *Chem. Soc. Rev.* **2010**, *39*, 2158–2183.

(21) Toledano, T.; Biller, A.; Bendikov, T.; Cohen, H.; Vilan, A.; Cahen, D., Controlling Space Charge of Oxide-Free Si by in Situ Modification of Dipolar Alkyl Monolayers. *J. Phys. Chem. C* **2012**, *116*, 11434-11443.

(22) Lai, B.-C.; Wu, J.-G.; Luo, S.-C., Revisiting Background Signals and the Electrochemical Windows of Au, Pt, and Gc Electrodes in Biological Buffers. *ACS Appl. Energy Mater.* **2019**, *2*, 6808–6816.
(23) Chatterjee, S.; Carter, R.; Oakes, L.; Erwin, W. R.; Bardhan, R.; Pint, C. L., Electrochemical and Corrosion Stability of Nanostructured Silicon by Graphene Coatings: Toward High Power Porous Silicon Supercapacitors. *J. Phys. Chem. C* **2014**, *118*, 10893–10902.
(24) Wu, Y. F.; Kashi, M. B.; Yang, Y.; Goncales, V. R.; Ciampi, S.; Tilley, R. D.; Gooding, J. J., Light-Activated Electrochemistry on Alkyne-Terminated Si(100) Surfaces Towards Solution-Based Redox Probes. *Electrochim Acta* **2016**, *213*, 540–546.
(25) Marrani, A. G.; Zanoni, R.; Schrebler, R.; Dalchiele, E. A., Toward Graphene/Silicon Interface Via Controlled Electrochemical Reduction of Graphene Oxide. *J. Phys. Chem. C* **2017**, *121*, 5675–5683.
(26) Shougee, A.; Konstantinou, F.; Albrecht, T.; Fobelets, K., Cyclic Voltammetry Peaks Due to Deep Level Traps in Si Nanowire Array Electrodes. *Ieee T Nanotechnol* **2018**, *17*, 154–160.
(27) Ferrie, S.; Darwish, N.; Gooding, J. J.; Ciampi, S., Harnessing Silicon Facet-Dependent Conductivity to Enhance the Direct-Current Produced by a Sliding Schottky Diode Triboelectric Nanogenerator. *Nano Energy* **2020**, *78*, 105210.
(28) Norman, L. L.; Badia, A., Redox Actuation of a Microcantilever Driven by a Self-Assembled Ferrocenylundecanethiolate Monolayer: An Investigation of the Origin of the Micromechanical Motion and Surface Stress. *J. Am. Chem. Soc.* **2009**, *131*, 2328-2337.
(29) Yang, Y.; Ciampi, S.; Choudhury, M. H.; Gooding, J. J., Light Activated Electrochemistry: Light Intensity and Ph Dependence on Electrochemical Performance of Anthraquinone Derivatized Silicon. *J. Phys. Chem. C* **2016**, *120*, 2874–2882.
(30) Devaraj, N. K.; Dinolfo, P. H.; Chidsey, C. E. D.; Collman, J. P., Selective Functionalization of Independently Addressed Microelectrodes by Electrochemical Activation and Deactivation of a Coupling Catalyst. *J. Am. Chem. Soc.* **2006**, *128*, 1794-1795.
(31) Cerofolini, G. F.; Galati, C.; Renna, L., Accounting for Anomalous Oxidation States of Silicon at the Si/SiO_2 Interface. *Surf. Interface Anal.* **2002**, *33*, 583-590.
(32) Nohira, T.; Yasuda, K.; Ito, Y., Pinpoint and Bulk Electrochemical Reduction of Insulating Silicon Dioxide to Silicon. *Nat. Mater.* **2003**, *2*, 397-401.
(33) Yasuda, K.; Nohira, T.; Takahashi, K.; Hagiwara, R.; Ogata, Y. H., Electrolytic Reduction of a Powder-Molded SiO_2 Pellet in Molten $CaCl_2$ and Acceleration of Reduction by Si Addition to the Pellet. *J. Electrochem. Soc.* **2005**, *152*, D232–D237.
(34) Yasuda, K.; Nohira, T.; Hagiwara, R.; Ogata, Y. H., Direct Electrolytic Reduction of Solid SiO_2 in Molten $CaCl_2$ for the Production of Solar Grade Silicon. *Electrochim. Acta* **2007**, *53*, 106–110.
(35) Yang, J. M.; Park, J. C.; Park, Y. B.; Kim, J. J.; Back, T. S.; Lee, H. S.; Lee, S. Y.; Park, S. W., Analytical Electron Microscopy Study of Nanometre - Scale Oxide Formed in Contact - Hole - Bottom Si Surfaces. *J. Electron. Microsc.* **2003**, *52*, 305 – 308.
(36) Inoue, S.; Ichinohe, M.; Sekiguchi, A., The Isolable Cation Radical of Disilene: Synthesis, Characterization, and a Reversible One-Electron Redox System. *J. Am. Chem. Soc.* **2008**, *130*, 6078-6079.
(37) Tan, C.-S.; Hsieh, P.-L.; Chen, L.-J.; Huang, M. H., Silicon Wafers with Facet-Dependent Electrical Conductivity Properties. *Angew. Chem. Int. Ed.* **2017**, *56*, 15339–15343.
(38) Vogel, Y. B.; Zhang, J.; Darwish, N.; Ciampi, S., Switching of Current Rectification Ratios within a Single Nanocrystal by Facet-Resolved Electrical Wiring. *ACS Nano* **2018**, *12*, 8071–8080.
(39) Allongue, P.; Henry de Villeneuve, C.; Morin, S.; Boukherroub, R.; Wayner, D. D. M., The Preparation of Flat H-Si(111) Surfaces in 40% Nh_4f Revisited. *Electrochim. Acta* **2000**, *45*, 4591–4598.
(40) Rijksen, B.; Pujari, S. P.; Scheres, L.; van Rijn, C. J. M.; Baio, J. E.; Weidner, T.; Zuilhof, H., Hexadecadienyl Monolayers on Hydrogen-Terminated Si(111): Faster Monolayer Formation and Improved Surface Coverage Using the Enyne Moiety. *Langmuir* **2012**, *28*, 6577-6588.
(41) O'Leary, L. E.; Rose, M. J.; Ding, T. X.; Johansson, E.; Brunschwig, B. S.; Lewis, N. S., Heck Coupling of Olefins to Mixed Methyl/Thienyl Monolayers on Si(111) Surfaces. *J. Am. Chem. Soc.* **2013**, *135*, 10081-10090.
(42) Cho, S. K.; Fan, F.-R. F.; Bard, A. J., Formation of a Silicon Layer by Electroreduction of SiO_2 Nanoparticles in $CaCl_2$ Molten Salt. *Electrochim. Acta* **2012**, *65*, 57–63.
(43) Schmidt, P. F.; Ashner, J. D., Tracer Investigation of Hydroxyls in Sio_2 Films on Silicon. *J. Electrochem. Soc.* **1971**, *118*, 325.
(44) DiMaria, D. J.; Cartier, E.; Arnold, D., Impact Ionization, Trap Creation, Degradation, and Breakdown in Silicon Dioxide Films on Silicon. *J. Appl. Phys.* **1993**, *73*, 3367-3384.
(45) Mihaychuk, J. G.; Shamir, N.; van Driel, H. M., Multiphoton Photoemission and Electric-Field-Induced Optical Second-Harmonic Generation as Probes of Charge Transfer across the Si/SiO_2 Interface. *Phys. Rev. B* **1999**, *59*, 2164–2173.
(46) Zhang, X. G., *Electrochemistry of Silicon and Its Oxide*. Kluwer Academic, New York,, **2001**.
(47) Uritsky, V. X., Role of Electron / Hole Processes in the Initial Stage of Silicon Anodization. *Mater. Sci. Forum* **1995**, *185-188*, 115-118.
(48) Young, L.; Zobel, F. G. R., An Ellipsometric Study of Steady-State High Field Ionic Conduction in Anodic Oxide Films on Tantalum, Niobium, and Silicon. *J. Electrochem. Soc.* **1966**, *113*, 277.
(49) Jakubowicz, J., Study of Surface Morphology of Electrochemically Etched N-Si (111) Electrodes at Different Anodic Potentials. *Cryst. Res. Technol.* **2003**, *38*, 313–319.
(50) Lee, J. Y.; Lee, J. G.; Lee, S. H.; Seo, M.; Piao, L.; Bae, J. H.; Lim, S. Y.; Park, Y. J.; Chung, T. D., Hydrogen-Atom-Mediated Electrochemistry. *Nat. Commun.* **2013**, *4*, 2766.
(51) Mackintosh, W. D.; Plattner, H. H., The Identification of the Mobile Ion During the Anodic Oxidation of Silicon. *J. Electrochem. Soc.* **1977**, *124*, 396-400.

SYNOPSIS TOC

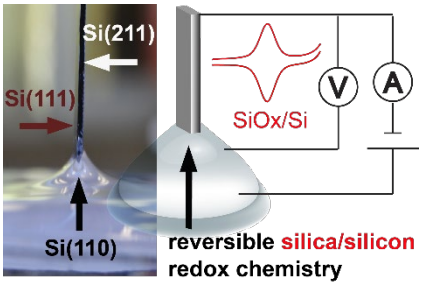

Facet-resolved electrochemistry, and conductive atomic force microscopy, reveal that traces of silica grown on highly conductive Si(110) crystal facets leads to reversible electrochemical silica-to-silicon reduction. Minor oxidative damaging of nominal single crystal electrodes causes parasitc signals whose origin is now explained as the room-temperature reversible silica–silicon redox conversion.